FLOW AND HEAT TRANSFER OF A FLUID-PARTICLE SUSPENSION PAST A VERTICAL EXPONENTIALLY STRETCHING SURFACE

G.M. PAVITHRA[1] & SUBRAMANYA KILARKAJE [2]

[1]Department of Mathematics, Sahyadri Science College, Kuvempu University, Shankaraghatta-577 451, Shimoga, Karnataka, INDIA.

[2] Department of Physics, Sahyadri Science College, Kuvempu University, Shankaraghatta-577 451, Shimoga, Karnataka, INDIA.

Abstract:

The article discusses the impact of internal heat generation/absorption and viscosity dissipation on the two-dimensional boundary layer stable flow and heat transfer of an incompressible viscous dusty fluid in the presence of a transverse magnetic field. The boundary condition equations are translated into a list of non ordinary differential equations and numerically solved using the Runge-Kutta-Fehlberg 45 technique using the Maple software. Prescribed exponential order surface temperature (PEST) and prescribed exponential order heat flux at the sheet are the two situations examined for heat transfer analysis (PEHF). The numerical results obtained are compared to those from the previous study and found to be in great agreement. The effect of the various parameters in the problem just on velocity and temperature profiles is deduced, discussed quantitatively for various physical parameter values, and displayed in graphs and tables.

Keywords: Numerical solution, fluid-particle suspension, exponentially stretching sheet,

Internal heat generation/absorption

1. Introduction

The analysis of boundary layer flow has a variety of applications, including aerodynamic extraction of a plastic sheet, cooling a metallic plate inside a cooling bath, the boundary layer across material handling conveyers, blood flow difficulties, and the textile and paper industries, among others. Sakiadis [1] pioneered the concept of boundary layer flow driven by the a continuously moving solid surface, and a substantial body of work has been developed on boundary layer flow of Newtonian & non-Newtonian fluids over linear and nonlinear stretching surfaces. Crane [2] extended his work by developing an analytical solution for the steady two-dimensional free convection flow past a stretched plate. Sharidan et al. [3] found the solution for an unstable boundary layer flow and heat transfer caused by a stretching sheet. Subhas Abel et al. [4] studied the influence of viscous dissipation and a non-uniform heat source on the boundary layer flow and heat transmission of a visco-elastic fluid over a stretching. Elbashbeshy and Aldawody [5] examined the influence of thermal radiation and a magnetic field on unstable mixed convection heat and mass transfer across a porous stretched surface.

Later on, this topic was expanded to include linear, non-linear, exponential stretching sheets with magnetohydrodynamic effects, porous sheets, porous media, and heat or mass transfer in both steady and unsteady flow scenarios. Numerous experts have since conducted exhaustive studies on the exponential stretching sheet. Magyari and Keller [6] initially proposed an exponential stretching model of boundary layer flow with a temperature distribution that is exponential. Al-Odat et al. [7] numerically examined the boundary layers flow on an exponentially stretching continuous line with an exponential temperature distribution with in presence of a magnetic field influence and provided a local similarity solution for an exponentially stretching surface. By addressing the thermal radiation impact, Bidin and Nazar [8] solved numerically the boundary layer flow issue over an exponentially stretched sheet. Nadeem et al. [9] examined the convective flow of a Jeffrey fluid across an exponentially extending surface and obtained an analytical solution through the use of homotopy analysis (HAM). Mukhopadhyay [10] and [11] find the numerical solution by taking into account the impact of MHD, heat radiation, and slip impacts on permeable boundary layer flow caused by an exponentially stretched sheet. Kameswaran et al. [12] recently explored the radiation impact on hydromagnetic Newtonian liquid flow caused by an exponential stretching sheet.

The experiment described above is limited to the flow and heat transfer of fluids caused by a horizontal stretching sheet. MHD free-convection flows are technologically significant for applications in the disciplines of stellar & planetary magnetospheres, aeronautics, chemical engineering, and electronics. Mixed convection flows are critical when buoyancy forces exert a considerable influence on the flow and thermal fields as a result of the large temperature differential between the wall as well as the ambient fluid. Partha et al. [13] conducted one of the earliest investigations toward a vertical surface, discussing the viscous dissipation effect for boundary layer flow across an exponentially stretching sheet and discovering that the non-dimensional friction factor increases as a result of viscous dissipation in the medium. El-Aziz [14] investigated the boundary-layer flow and heat transmission properties of a heated exponential extending continuous sheet that was cooled by a mixed convection flow. Reddy and Reddy [15] investigated the effect of thermal radiation on hydro-magnetic flow caused by an exponentially stretched sheet. Dulal Pal [16] investigated mixed convection heat transfer in boundary layers on an exponentially extending continuous surface in the presence of a magnetic field and compared his findings to those obtained by [5] and [6]. Srinivasacharya and RamReddy conducted a study to investigate the combined impacts of Soret and Dufour upon mixed convection over an exponentially stretched sheet [17]. El-Aziz and Tamer Nabil [18] discovered the analytical solution for hydromagnetic mixed convection flow across an exponentially stretched sheet with hall current using the Homotopy analysis approach.

Fluid mechanics problems involving dust particles arise in a wide variety of practical processes, including flow in powder technology, transport of liquid slurries in chemical processing, nuclear processing, fluidization, combustion, dust use in gas cooling applications, centrifugal separation of matter from fluid, petroleum industry, flow in rocket tubes, crude oil purification, electrostatic precipitation, polymer technology, and fluid draught. Saffman [19] initiated the flow relating the fluid-particle system for laminar flow of a dusty fluid. Ghosh [20] investigated the hydromagnetic flow of the a dusty viscoelastic Maxwell fluid via a rectangular channel for just an arbitrary pressure gradient based on this work. Chamkha [21] develops a two-phase fluid–particle model that accounts for fluid-phase heat production or absorption as well as thermal radiation and applies it to the problem of heat transmission in a particulate suspension flow over a heated horizontal surface in the presence of a gravity field. Later, Ezzat et al. [22] generalised the problem of dusty fluid hydro-magnetic flow across a porous medium. Again, Attia et al [23] investigated an unsteady Couette flow with heat exchange of a viscous incompressible electrically conducting fluid that under effect of an exponentially diminishing pressure gradient. Gireesha et al. ([24], [25]) have recently discussed the effect of variable viscosity and heat source/sink on the MHD boundary layer flow and & heat transfer of a dusty fluid over an unstable stretched sheet.

We have focussed our efforts on the flow and heat transfer properties near to a vertical stretched sheet as a result of our experiments. This problem is distinct from the previous investigations, which did not examine the exponential stretching sheet for dusty fluid. This article discusses the effects of suction or injection on an exponential stretching surface. Using similarity transformations, a third order ordinary differential equation representing the momentum equation as well as a second order differential equation representing the energy equation are generated. The Runge-Kutta-Fehlberg 45 technique was used to do numerical computations up to the necessary level of precision for various values of the problem's dimensionless parameters with the goal of graphically showing the findings.

2. Mathematical Formulation and Solution of the Problem

Consider a steady two-dimensional laminar boundary layer flow and heat transfer of an incompressible viscous dusty fluid near a vertical wall stretching with velocity U_w and temperature distribution T_w. It is assumed that the surface is stretched with exponential velocity $U_w = U_0 e^{(x/L)}$ in quiescent fluid and the surface is maintained at a temperature $T_w = T_1 + T_0 e^{(c_1 x/2L)}$. The x-axis is chosen along the sheet and y-axis normal to it. The flow is generated as a consequence of exponential stretching of the sheet, caused by simultaneous application of equal and opposite forces along the x-axis keeping in which the origin fixed as in the Figure 1. A uniform magnetic field B is assumed to be applied in the y-direction and suction/injection S is applied normal to the sheet.

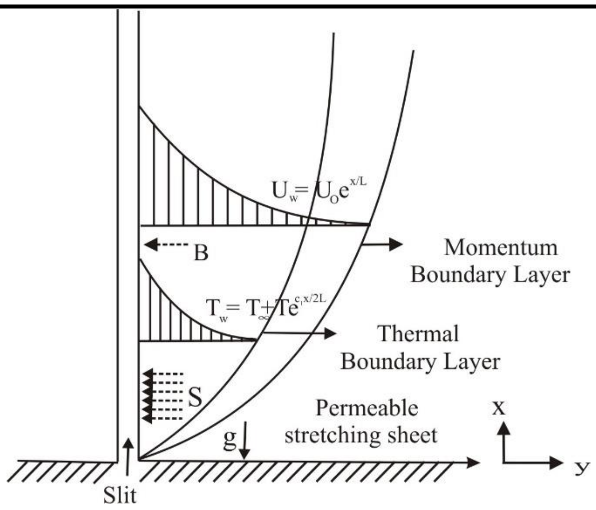

Figure 1: Schematic representation of the boundary layer flow.

Under these assumptions, the two dimensional boundary layer equations can be written as,

$$\frac{\partial u}{\partial x}+\frac{\partial v}{\partial y}=0, \tag{2.1}$$

$$u\frac{\partial u}{\partial x}+v\frac{\partial u}{\partial y}=\nu\frac{\partial^2 u}{\partial y^2}+\frac{KN}{\rho}(u_p-u), \tag{2.2}$$

$$\frac{\partial u_p}{\partial x}+\frac{\partial v_p}{\partial y}=0, \tag{2.3}$$

$$u_p\frac{\partial u_p}{\partial x}+v_p\frac{\partial u_p}{\partial y}=\frac{K}{m}(u-u_p), \tag{2.4}$$

where x and y represents coordinate axes along the continuous surface in the direction of motion and perpendicular to it, respectively. (u,v) and (u_p,v_p) denotes the velocity components of the fluid and particle phase along the x and y directions respectively, T is the temperature of the fluid, T_∞ is the temperature of the fluid far away from the sheet, g is the acceleration due to gravity, β^* is the thermal expansion coefficient, ν is the coefficient of viscosity of fluid, ρ is the density of the fluid phase, K is the Stoke's resistance, N is the number density of dust particles, m is the mass concentration of dust particles, $\tau_v=m/K$ is the relaxation time of particle phase and σ is the electrical conductivity.

In order to solve the governing boundary layer equations, consider the following appropriate boundary conditions on velocity,

$$u=U_w(x),\qquad v=V_w(x)\qquad \text{at } y=0,$$

$$u\to 0,\qquad u_p\to 0,\qquad v_p\to 0,\qquad \text{as } y\to\infty, \tag{2.5}$$

where $U_w(x)=U_0e^{(x/L)}$ is the sheet velocity and $V_w(x)=-S\sqrt{U_0\nu/2L}e^{(x/2L)}$ is the suction/ injection velocity, U_0 is reference velocity, L is the reference length and S is the suction/injection parameter. It should be noted that $S>0$ corresponds to fluid wall suction while $S<0$ indicates fluid wall injection.

Equations (2.1) to (2.4) are subjected to boundary condition (2.5), admit a self-similar solution in terms of the similarity function f and the similarity variable η as

$$u = U_0 e^{\frac{x}{L}} f'(\eta), \qquad v = -\sqrt{\frac{u_0 \nu}{2L}} e^{\frac{x}{2L}} [f(\eta) + \eta f'(\eta)],$$

$$u_p = U_0 e^{\frac{x}{L}} F'(\eta), \qquad v_p = -\sqrt{\frac{u_0 \nu}{2L}} e^{\frac{x}{2L}} [F(\eta) + \eta F'(\eta)],$$

$$\eta = \sqrt{\frac{u_0}{2\nu L}} e^{\frac{x}{2L}} y \qquad B = B_0 e^{\frac{x}{2L}}, \qquad \theta(\eta) = \frac{T - T_\infty}{T_w - T_\infty}, \tag{2.6}$$

where B_0 is the magnetic field flux density.

These equations identically satisfy the governing equations (2.1) and (2.2). Substitute equation (2.5) into equations (2.1) and (2.3) and on equating the coefficient of $(x \setminus L)^0$ on both sides one can get

$$f'''(\eta) + f(\eta) f''(\eta) - 2f'(\eta)^2 + 2l\beta[F'(\eta) - f'(\eta)] - Mf'(\eta) + 2Gr\,\theta(\eta) = 0 \tag{2.7}$$

$$F(\eta)F''(\eta) - 2F'(\eta)^2 + 2\beta[f'(\eta) - F'(\eta)] = 0, \tag{2.8}$$

where prime denotes the differentiation with respect to η and $l = mN/\rho$ is the mass concentration, $\beta = L/\tau_v U_0$ is the fluid-particle interaction parameter for velocity, $M = 2\sigma B_0^2 L/\rho U_0$ is the magnetic parameter and $Gr = g\beta(T_w - T_\infty)L/U_0^2$ is the Grashof number.

Using similarity transformations, the boundary conditions (2.4) become

$$f'(\eta) = 1, \quad f(\eta) = S \quad \text{at } \eta = 0,$$

$$f'(\eta) = 0, \quad F'(\eta) = 0, \quad F(\eta) = f(\eta) + \eta f'(\eta) - \eta F'(\eta) \quad \text{as } \eta \to \infty, \tag{2.9}$$

The important physical parameter for the boundary layer flow is the skin-friction coefficient which is defined as,

$$C_f = \frac{\tau_w}{\rho U_w^2}, \tag{2.10}$$

where the skin friction τ_w is given by,

$$\tau_w = \mu\left(\frac{\partial u}{\partial y}\right)_{y=0}. \qquad (2.11)$$

Using the non-dimensional variables, one obtains,

$$\sqrt{2\,\mathrm{Re}\,C_f} = f''(0),$$

where $\mathrm{Re} = \dfrac{U_0 L}{\nu}$ is the Reynolds number.

3. Heat Transfer Analysis

The governing steady, boundary layer heat transport equations with internal heat generation/absorption and viscous dissipation are given by,

$$\rho c_p\left[u\frac{\partial T}{\partial x} + v\frac{\partial T}{\partial y}\right] = k\frac{\partial^2 T}{\partial y^2} + \frac{Nc_p}{\tau_T}(T_p - T) + \frac{N}{\tau_v}(u_p - u)^2 + \mu\left(\frac{\partial u}{\partial y}\right)^2 + Q(T - T_\infty), \quad (3.1)$$

$$Nc_m\left[u_p\frac{\partial T_p}{\partial x} + v_p\frac{\partial T_p}{\partial y}\right] = -\frac{Nc_p}{\tau_T}(T_p - T), \qquad (3.2)$$

where T and T_p are the temperatures of the fluid and dust particle inside the boundary layer, c_p and c_m are the specific heat of fluid and dust particles, τ_T is the thermal equilibrium time i.e., it is time required by a dust cloud to adjust its temperature to the fluid, k is the thermal conductivity, τ_v is the relaxation time of the of dust particle i.e., the time required by a dust particle to adjust its velocity relative to the fluid and Q represents the heat source when $Q > 0$ and the sink when $Q < 0$.

We have consider the heat transfer phenomenon for two types of heating process, namely

(1) Prescribed exponential order surface temperature (PEST) and

(2) Prescribed exponential order heat flux (PEHF).

Case 1: Prescribed Exponential Order Surface Temperature (PEST):

For this heating process, we employ the following boundary conditions,

$$T = T_w(x) \quad \text{at } y = 0,$$

$$T \to T_\infty, \quad T_p \to T_\infty \text{ as } y \to \infty, \qquad (3.3)$$

where $T_w = T_\infty + T_0 e^{c_1 x/2L}$ is the temperature distribution in the stretching surface, T_0 is a reference temperature and c_1 is a constant.

Introducing the dimensionless variables for the temperatures $\theta(\eta)$ and $\theta_p(\eta)$ as follows:

$$\theta(\eta)=\frac{T-T_\infty}{T_w-T_\infty}, \qquad \theta_p(\eta)=\frac{T_p-T_\infty}{T_w-T_\infty}, \tag{3.4}$$

where $T-T_\infty=T_0 e^{c_1 x/2L}\theta(\eta)$.

Using the similarity variable η and (3.4) into (3.1) and (3.2) and on equating the co-efficient of $(x\setminus L)^0$ on both sides, one can arrive the following system of equations;

$$\begin{aligned}&\theta''(\eta)+\Pr[f(\eta)\theta'(\eta)-c_1 f'(\eta)\theta(\eta)]+\frac{2N}{\rho}\beta_T \Pr[\theta_p(\eta)-\theta(\eta)]\\ &\quad+\frac{2N}{\rho}\beta \Pr Ec[F'(\eta)-f'(\eta)]^2+\Pr Ec[f''(\eta)]^2+2\Pr\lambda\theta(\eta)=0\end{aligned} \tag{3.5}$$

$$c_1 F'(\eta)\theta_p(\eta)-F(\eta)\theta_p'(\eta)+2\beta_T\gamma[\theta_p(\eta)-\theta(\eta)]=0 \tag{3.6}$$

where $\Pr=\mu c_p/k$ is the Prandtl number, $Ec=U_0^2/c_pT$ is the Eckert number, $\lambda=QL^2/\mu C_p \operatorname{Re}$ is the heat source/sink parameter, $\beta=L/\tau_v U_0$ and $\beta_\tau=L/\tau_T U_0$ are the fluid-particle interaction parameter for velocity and temperature respectively and $\gamma=c_p/c_m$ is the ratio of specific heat.

The corresponding thermal boundary conditions become,

$$\begin{aligned}&\theta(\eta)=1 \quad \text{at } \eta=0,\\ &\theta(\eta)\to 0, \quad \theta_p(\eta)\to 0, \quad \text{as } \eta\to\infty.\end{aligned} \tag{3.7}$$

Case 2: Prescribed Exponential Order Heat Flux (PEHF):

For this heating process, the boundary conditions are considered as,

$$\begin{aligned}&\frac{\partial T}{\partial y}=-\frac{q_w(x)}{k} \quad \text{at } y=0,\\ &T\to T_\infty, \quad T_p\to T_\infty \quad \text{as } \eta\to\infty,\end{aligned} \tag{3.8}$$

where $q_w(x)=T_1 e^{(c_1+1)x/2L}$, T_1 is reference temperature.

Again using the similarity variable η and equation (3.4) into equations (3.1) and (3.2) and by equating the co-efficient $(x\setminus L)^0$ on both sides, we get the system of equations as in the equations (3.5) and (3.6) with $Ec=kU_0^2/c_pT_1\sqrt{U_0/2\nu L}$, which is different from the PEST case, and all other parameters are the same as in PEST case.

The corresponding thermal boundary conditions become,

$$\begin{aligned}&\theta'(\eta)=-1 \quad \text{at } \eta=0,\\ &\theta(\eta)\to 0, \quad \theta_p(\eta)\to 0, \quad \text{as } \eta\to\infty\end{aligned} \tag{3.9}$$

The important physical parameter for the heat transfer coefficient which is defined as,

$$Nu_x = \frac{xq_w}{k(T_w - T_\infty)}, \tag{3.10}$$

where the heat transfer from the sheet q_w is given by,

$$q_w = -k\left(\frac{\partial T}{\partial y}\right)_{y=0}. \tag{3.11}$$

Using the non-dimensional variables, one obtains,

$$\frac{Nu_x}{\sqrt{2\,\mathrm{Re}}} = -\frac{x}{2L}\theta'(0),\ \text{(PEST case)} \quad \text{and} \quad \frac{Nu_x}{\sqrt{2\,\mathrm{Re}}} = -\frac{x}{2L}\frac{1}{\theta(0)}\ \text{(PEHF case)}.$$

4. Numerical Solution

The non-linear differential equations (2.6)-(2.7), (3.5)-(3.6) for both PEST and PEHF cases have been solved numerically by applying Runge-Kutta-Fehlberg 45. We have chosen suitable finite value of $\eta \to \infty$ as $\eta = 5$.

Table 1: Comparison of the results of skin friction coefficient $f''(0)$ for various values of M with $c_1 = 4$ and $\beta = N = S = 0$.

M	Reddy and Reddy [14]	Kameswaran et al. [11]	Present Study
0	-1.28213	-1.28213	-1.28213
1.0	-1.62918	-1.62918	-1.62918
2.0	-	-1.91262	-1.91262
3.0	-	-2.15874	-2.15873
4.0	-	-2.37937	-2.37936

Table 2: Comparison of the results of $-\theta'(0)$ for various values of $\Pr$ with $c_1 = 1$ and $\beta = N = S = 0$

Pr	Swati et al. [9]	Mohamed et al. [17]	Present Study
1	0.9547	0.9553	0.9550
2	1.4714	-	1.4714
3	1.8691	1.8693	1.8692
5	2.5001	2.5003	2.5003
10	3.6603	3.6739	3.6603

Tables 1 and 2 provide the values of the skin-friction coefficient and heat transfer coefficient for different values of the magnetic parameter M and Prandtl number $\Pr$. In order to assess the accuracy of the method, the results of $f''(0)$ are compared with those obtained by Reddy and Reddy [14] and Kameswaran et al. [11] in the absence of fluid-particle interaction parameter and Number of dust particles. Also, there is a comparison of our results of $-\theta'(0)$ with Mukhopadhyay et al. [9] and

Mohamed et al. [17] as in Table 2 for various values of $\Pr$. From these two tables, one can notice that there is a close agreement with this approach and thus verifies the accuracy of the method used.

Table 3: Values of wall temperature gradient $\theta'(0)$ (for PEST case) and wall temperature $\theta(0)$ (for PEHF case) with $S = 2$.

β	M	Gr	λ	Pr	Ec	N	$-f''(0)$	$\theta'(0)$ (PEST)	$\theta(0)$ (PEHF)
0.2							-1.26625	-0.81099	1.14763
0.6	1.0	1.0	0.5	0.72	0.5	0.5	-1.27862	-0.79106	1.16386
1.0							-1.28809	-0.78371	1.16981
	1.0						-1.27862	-0.79106	1.16386
0.6	2.0	1.0	0.5	0.72	0.5	0.5	-1.61308	-0.67804	1.25833
	3.0						-1.90379	-0.57357	1.35028
		1.0					-1.27862	-0.79106	1.16386
0.6	1.0	2.0	0.5	0.72	0.5	0.5	-0.53159	-0.97643	1.01716
		3.0					0.16055	-1.06425	0.95327
			-0.5				-1.52123	-1.53098	0.71665
0.6	1.0	1.0	0	0.72	0.5	0.5	-1.43730	-1.22788	0.85795
			0.5				-1.27862	-0.79106	1.16386
				0.72			-1.27862	-0.79106	1.16386
0.6	1.0	1.0	0.5	1.0	0.5	0.5	-1.38569	-1.01091	0.99324
				1.5			-1.52185	-1.37994	0.82769
					0		-1.32531	-1.00710	0.99394
0.6	1.0	1.0	0.5	0.72	0.5	0.5	-1.27862	-0.79106	1.16386
					1.0		-1.23346	-0.59245	1.30152
						0.5	-1.278623	-0.79106	1.16386
0.6	1.0	1.0	0.5	0.72	0.5	1.0	-1.361391	-0.98772	1.00853
						1.5	-1.420032	-1.14726	0.90725

Further, we have studied the effects of fluid-particle interaction parameter (β), magnetic parameter (M), Grashof number (Gr), suction/injection parameter (S), heat source/sink parameter (λ), number density (N), Prandtl number ($\Pr$) and Eckert number (Ec) on velocity and temperature profiles and are depicted graphically. The thermal characteristics at the wall are examined for the values of skin-friction coefficient $f''(0)$, temperature gradient $\theta'(0)$ in PEST case and the temperature $\theta(0)$ in PEHF case are also tabulated in Table 3.

5. Results and Discussion

For the purpose of discussing the result, the numerical calculations are presented in the form of non-dimensional velocity and temperature profiles. Numerical computations have been carried out for different values of the pertinent parameters. The numerical values are plotted in Figures 2-5 for the velocity profiles and Figures 6-15 for the temperature profiles. We have used the values of $Ec = 0.6$, $M = N = S = 1.0$, $\Pr = 0.72$, $\beta = \beta_T = 0.6$, $c_1 = 1$, $\lambda = 0.5$, $Gr = 2.0$, $\rho = 1$ and $l = 0.1$ throughout our analysis.

Figure 2 reveals the effect of the fluid-particle interaction parameter (β) on the velocity profiles $f'(\eta)$ and $F'(\eta)$. It is noticed from this figure that the velocity profiles decrease with increasing values of β for the fluid phase and increase for the dust phase in the boundary layer. The effect of increasing the values of β is to reduce the velocity $f'(\eta)$ and thereby increase the boundary layer thickness as in Figure 2. In Figure 3, the velocity profiles are drawn for different values of the suction/injection parameter (S). It is observed that the velocity decreases significantly with increasing values of the suction parameter whereas it increases with the injection for both the fluid and dust phases so that the momentum boundary layers become thinner.

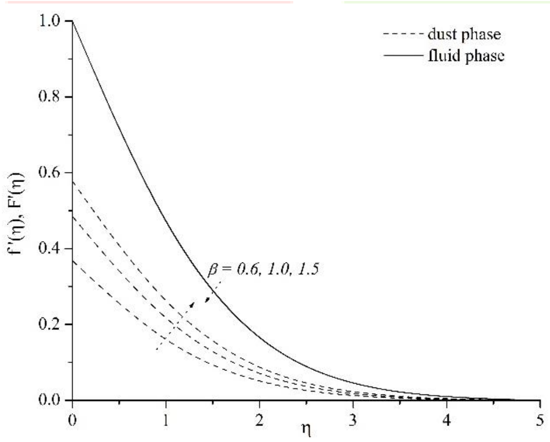

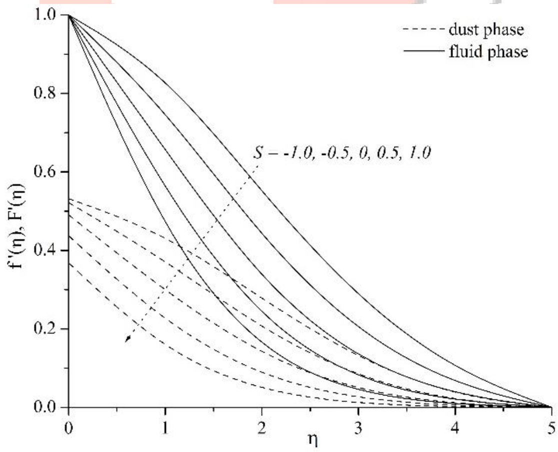

Figure 2: Effect of β on velocity profiles **Figure 3: Effect of S on velocity profiles.**

The effect of the magnetic parameter (M) on the velocity profiles for the fluid and dust phases are plotted in Figure 4. It explains that as the magnetic field parameter (M) increases, the velocity profile decreases. This is due to the fact that, the introduction of a transverse magnetic field (normal to the flow direction) has a tendency to create a drag, known as the Lorentz force which results in resisting the flow. Figure 5 exhibits the velocity profiles for various values of the Grashof number (Gr). From this figure, we see that the momentum boundary layer thickness reduces due to the increase of the velocity profile for an increase in the Grashof number (Gr).

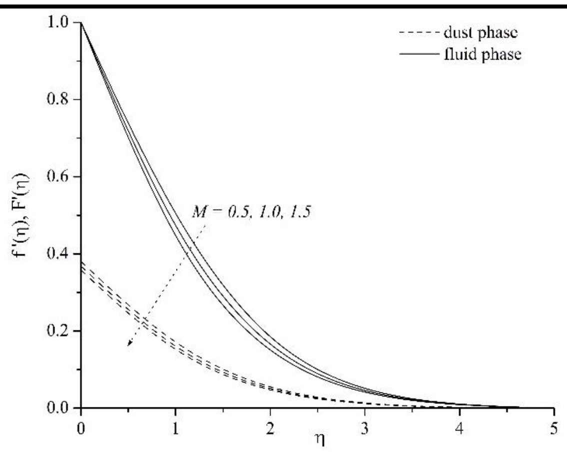

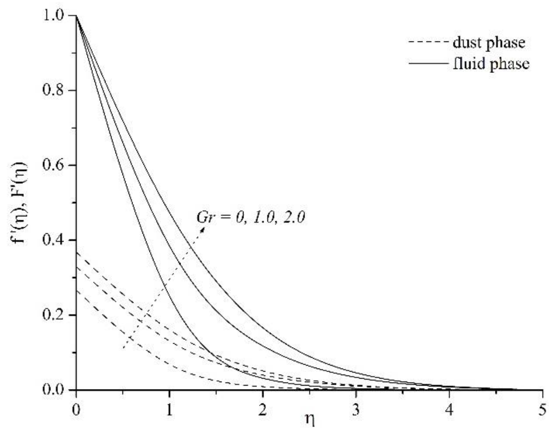

Figure 4: Effect of M on velocity profiles. **Figure 5: Effect of Gr on velocity profiles.**

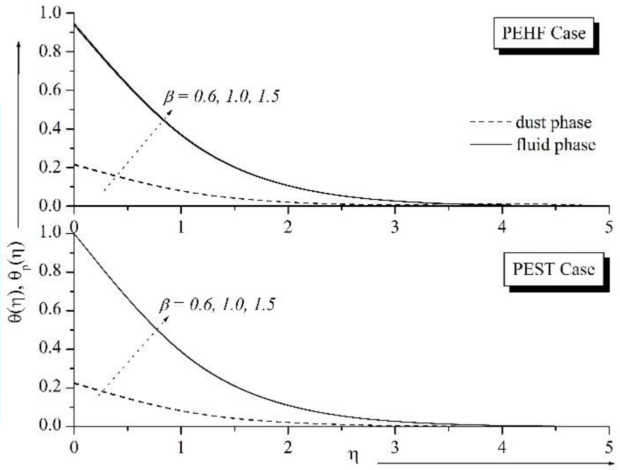

Figure 6: Effect of β on temperature profiles for PEST & PEHF cases.

The temperature profiles for different values of the fluid-particle interaction parameter (β) for both PEST and PEHF cases are presented in Figure 6. This figure shows that there is an increase in the temperature as the fluid-particle interaction parameter (β) increases. The effect of the magnetic field parameter (M) on the temperature profiles $\theta(\eta)$ and $\theta_p(\eta)$ for both PEST and PEHF cases are depicted as in Figure 7. From this figure, we observe that the temperature profiles increase with increases in the magnetic field parameter and also it indicates that both the fluid and the dust phase temperatures are parallel to each other. This is true for both PEST and PEHF cases.

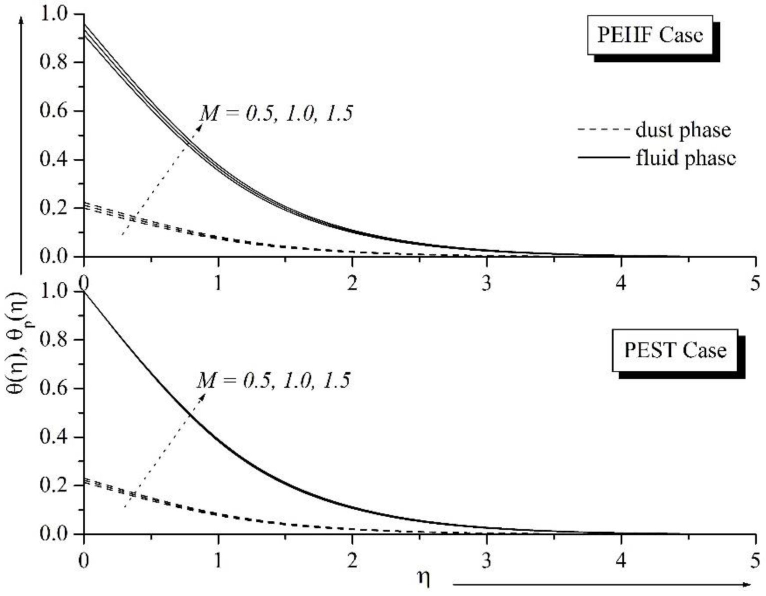

Figure 7: Effect of M on temperature profiles for PEST & PEHF cases.

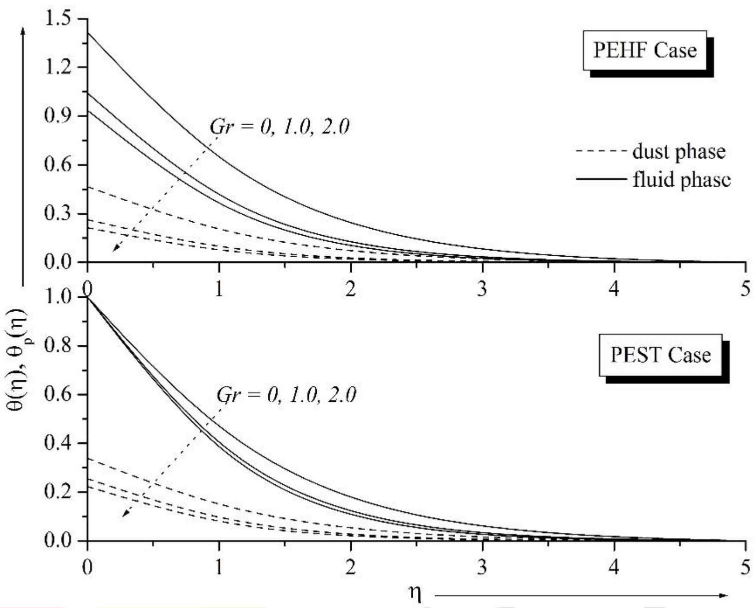

Figure 8: Effect of Gr on temperature profiles for PEST & PEHF cases.

The variation in the temperature for different values of the Grashof number (Gr) for PEST and PEHF cases are plotted in Figure 8. It is noted that when the Grashof number $Gr = 0$, the flow becomes a forced convection flow and when the value of Gr increases, the temperature profiles decrease in both cases, and this results in decreasing the thermal boundary layer thickness and the flow becomes a free convection flow.

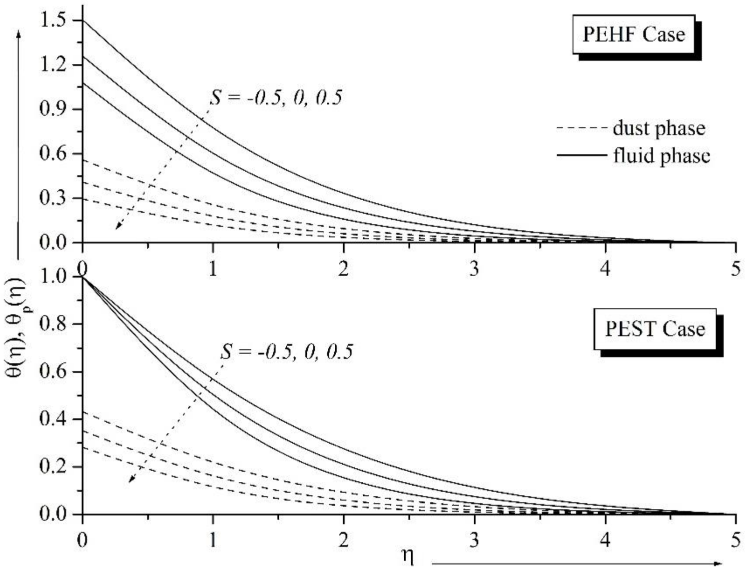

Figure 9: Effect of S on temperature profiles for PEST & PEHF cases.

Figure 9 presents the effect of the suction/injection parameter (S) on the temperature profiles for both PEST and PEHF cases. It reveals that the temperature decreases as the suction parameter increases which results in thinning of the thermal boundary layer thickness. However, by increasing the values of the injection parameter, the temperature increases with an increase in the thermal boundary layer thickness. Hence, suction can be used as a means for cooling the surface as it enhances the heat transfer coefficient much better than injection and thereby the thickness of the thermal boundary layer is reduced.

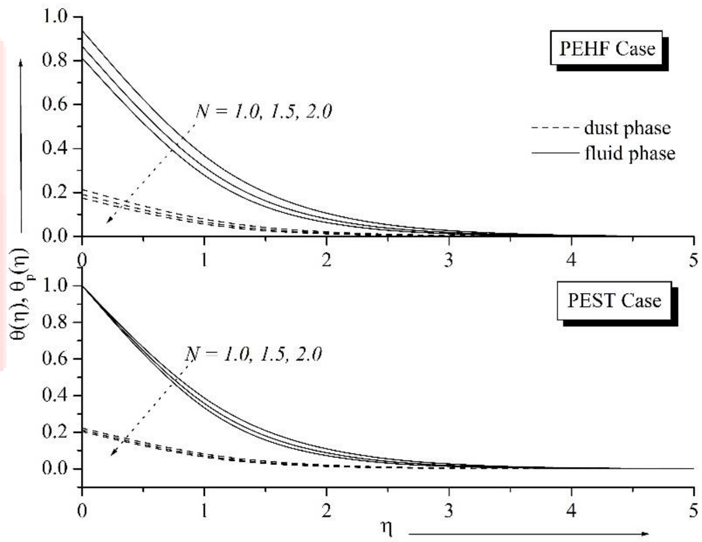

Figure 10: Effect of N on temperature profiles for PEST & PEHF cases.

Figure 10 shows the temperature distributions $\theta(\eta)$ and $\theta_p(\eta)$ for different values of the number density (N). We infer from this figure that the temperature decreases with increases in N for both cases. The effects of the heat source/sink parameter λ on the temperature profiles are observed in Figure 11. It shows that as λ increases, the temperature profiles for both the fluid and the dust phases increase for both PEST and PEHF cases.

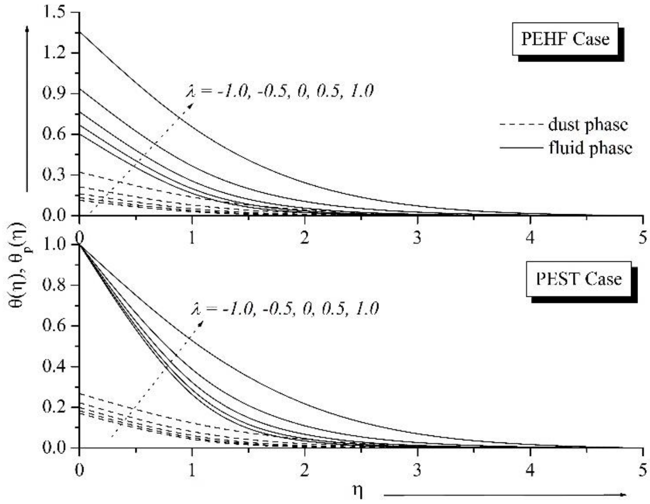

Figure 11: Effect of λ on temperature profiles for PEST & PEHF cases.

Figure 12 exhibits the role of the Prandtl number ($\Pr$) on the temperature profiles for both PEST and PEHF cases. In heat transfer problems, the Prandtl number controls the relative thickness of the momentum and thermal boundary layers. When $\Pr$ is small, it means that the heat diffuses very quickly when compared to the velocity (momentum). This means that for liquid metals the thickness of the thermal boundary layer is much bigger than the velocity boundary layer. Therefore, increasing the value of $\Pr$ results in a decrease in the temperature distribution and hence, the thermal boundary layer thickness decreases as $\Pr$ increases.

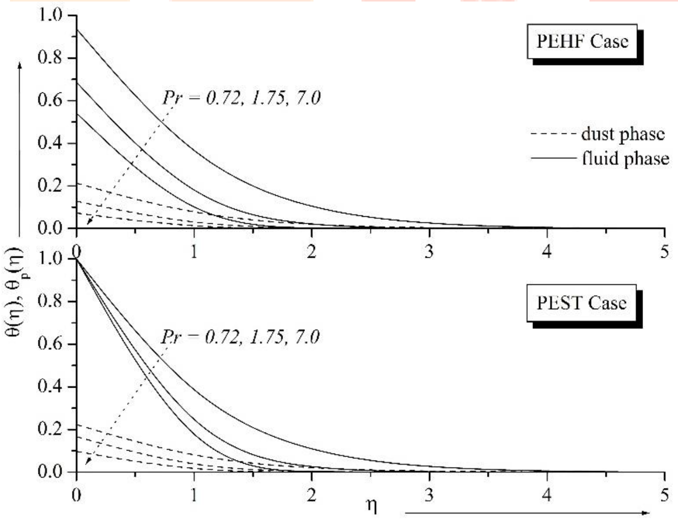

Figure 12: Effect of $\Pr$ on temperature profiles for PEST & PEHF cases.

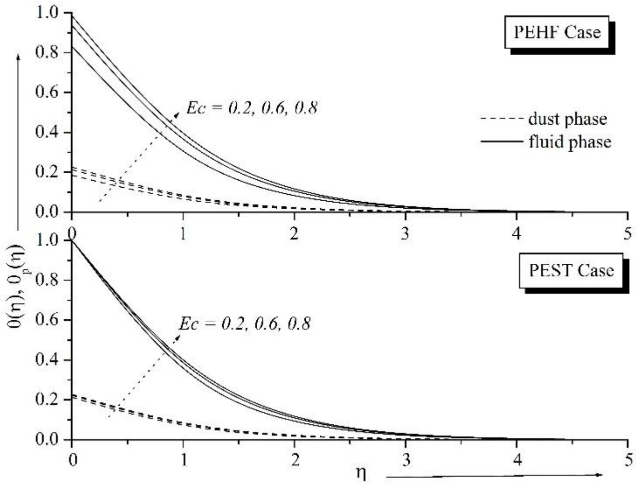

Figure 13: Effect of Ec on temperature profiles for PEST & PEHF cases.

Figure 13 depicts the effect of the Eckert number (Ec) on the temperature profiles with η. It can be seen from this figure that the temperature increases with increasing values of Ec because it plays a role like an energy source, which leads to affect the heat transfer rate. This is due to the heat energy stored in the liquid due to the frictional heating.

Figure 14 shows the variation of the skin friction $f''(0)$ verses the suction/injection parameter S for different values of the magnetic parameter (M) and the Grashof number (Gr), respectively. It can be noticed that the skin friction decreases with an increase in the magnetic parameter (M) and vice versa for the Grashof number (Gr).

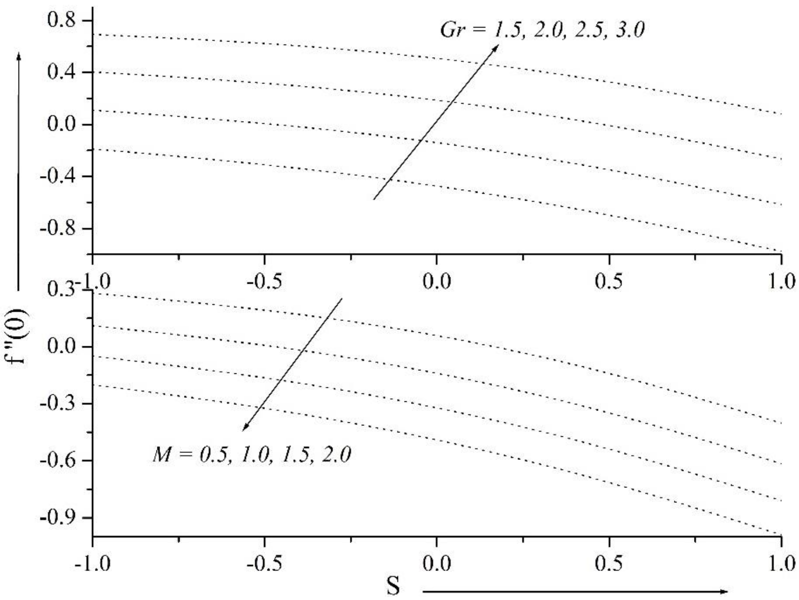

Figure 14: Effect of skin friction coefficient for different values of M and Gr vs S.

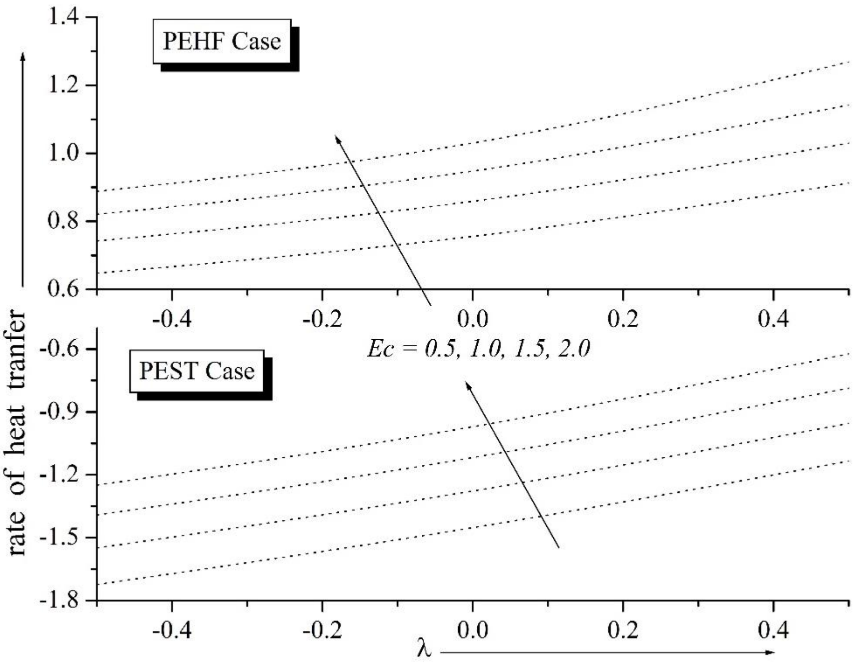

Figure 15: Effect of heat transfer on λ for PEST & PEHF cases.

The rate of heat transfer from the sheet is evaluated by the variation of temperature gradient function $\theta'(0)$ in PEST case and the temperature function $\theta(0)$ in PEHF case and is presented in Figure 15 for various values of Ec. It is observed from this figure that the rate of heat transfer increases with increases in Ec. It is also evident that $\theta'(0)$ is negative which means heat transfer and $\theta(0)$ is positive means heat absorption. Hence, a PEHF case is better suited for cooling process and this is also clear from Table 3.

6. Conclusions

A numerical study is performed to study the problem of hydromagnetic flow of an incompressible viscous dusty fluid over an exponentially stretching sheet in the presence of internal heat generation/absorption. The boundary layer equations governing the flow are reduced to ordinary differential equations using similarity transformations. Using a numerical technique, these equations are then solved to obtain the velocity and temperature distributions as well as the skin-friction coefficient and the Nusselt number for various flow parameters. The results obtained are compared with previously existing results and found to be in good agreement. The major findings from the present study can be summarized as follows:

- The fluid-phase temperature is higher than the dust-phase temperature both in PEST and PEHF cases.
- The velocity profile decreases for increasing values of the suction parameter and the magnetic parameter, but this trend is reversed for increasing values of the Grashof number.
- The effect of the fluid-particle interaction parameter is favourable for the dust-phase velocity and unfavourable for fluid-phase velocity.
- The combined and individual effects of the magnetic parameter, fluid-particle interaction parameter, heat source/sink parameter and the viscous dissipation parameter increase the heat transfer rates.
- The effect of the Grashof number on the temperature field is quite opposite to that of the velocity field.
- Fluid wall suction can be used for cooling the surface.
- The rate of heat transfer decreases due to the effects of N and $\Pr$.
- The skin friction decreases with an increase in M and vice versa for Gr.
- It is observed that $\theta'(0)$ is negative which means heat transfer and $\theta(0)$ is positive means heat absorption. Hence the PEHF case is better for cooling purpose.

References:

[1] Sakiadis.B.C, Boundary layer behaviour on continuous solid surface ii, boundary layer behaviuor on continuous flat surface, AIChE J., 7(2) (1961) 221-235.

[2] Crane.L.J, Flow past a stretching plate, Z. Angew. Math. Phy., 21(4) (1970) 645-647.

[3] Sharidan.S, Mahmood.T and Pop.I, Similarity solutions for the unsteady boundary layer flow and heat transfer due to a stretching sheet, Int. J. of Appl. Mechanics and engineering, 11(3) (2006) 647-654.

[4] Subhas Abel.M, Siddeshwar.P.G and Nandeppanavar.M.M, Heat transfer in a viscoelastic boundary layer flow over a stretching sheet with viscous dissipation and non-uniform heat source, Int. J. of Heat and Mass Transfer, 50 (2007) 960-966.

[5] Elbashbeshy.E.M.A and Aldawody.D.A, Effect of thermal radiation and magnetic field on unsteady mixed convection flow and heat transfer over a porous stretching surface, Int. J. of nonlinear sciences, 9(4) (2010) 448-454.

[6] Magyari.E and Keller.B, Heat and mass transfer in the boundary layers on an exponentially stretching continuous surface, J. Phys. D: Appl. Phys., 32 (1999) 577-585.

[7] Al-Odat.M.Q, Damseh.R.A and Al-Azab.T.A, Thermal boundary layer on an exponentially stretching continuous surface in the presence of magnetic field effect, Int. J. of Appl. Mech. Eng., 11(2) (2006) 289-299.

[8] Biliana Bidin and Roslinda Nazar, Numerical solution of the boundary layer flow over an exponentially stretching sheet with thermal radiation, Eur. J. Sci. Res., 33 (4) (2009) 710-717.

[9] Sohail Nadeem, Shehla Zaheer and Tiegang Fangand, Effects of thermal radiation on the boundary layer flow of a Jeffrey fluid over an exponentially stretching surface, Numer. Algor., 57 (2011) 187-205.

[10] Swati Mukhopadhyay and Rama Subba Reddy Gorla, Effects of partial slip on boundary layer flow past a permeable exponential stretching sheet in presence of thermal radiation, Heat Mass Transfer, 48 (2012) 1773-1781.

[11] Swati Mukhopadhyay, Slip effects on MHD boundary layer flow over an exponentially stretching sheet with suction/blowing and thermal radiation, Ain Shams Engineering Journal (Article in press), (2012).

[12] Kameswaran.P.K, Narayana.M, Sibanda.P and Makanda.G, On radiation effects on hydromagnetic Newtonian liquid flow due to an exponential stretching sheet, Boundary Value Problems, 1(105) (2012) 1-16.

[13] Partha.M.K, Murthy.P.V.S.N and Rajasekhar.G.P, Effect of viscous dissipation on the mixed convection heat transfer from an exponentially stretching surface, Heat and Mass Transfer, 41 (2005) 360-366.

[14] El-Aziz.M.A, Viscous dissipation effect on mixed convection flow of a micropolar fluid over an exponentially stretching sheet, Can. J. Phys., 87 (2009) 359-368.

[15] Bala Anki Reddy.P and Bhaskar Reddy.N, Thermal radiation effects on hydro-magnetic flow due to an exponentially stretching sheet, Int. J. of Appl. Math. Comput., 3(4) (2011) 300-306.

[16] Dulal Pal, Mixed convection heat transfer in the boundary layers on an exponentially stretching surface with magnetic field, Appl. Math. Comput., 217 (2010) 2356-2369.

[17] Srinivasacharya.D and Ch.RamReddy, Soret and dufour effects on mixed convection from an exponentially stretching surface, Int. J. of Nonlinear Science, 12(1) (2011) 60-68.

[18] Mohamed Abd El-Aziz and Tamer Nabil, Homotopy analysis solution of hydromagnetic mixed convection flow past an exponentially stretching sheet with hall current, Math. Probl. Eng., 2012 (2012) 26 pages.

[19] Saffman.P.G, On the stability of laminar flow of a dusty gas, J. Fluid Mechanics, 13 (1962) 120-128.

[20] Ghosh.B.C, On the hydromagnetic flow of a dusty viscoelastic Maxwell fluid through a rectangular channel, Int. J. Appl. Mech. Eng., 7 (2000) 591-618.

[21] Chamkha.A.J, Effects of heat absorption and thermal radiation on heat transfer in a fluid–particle flow past a surface in the presence of a gravity field, Int. J. of Thermal Sciences, 39 (5) (2000) 605–615.

[22] Ezzat.M.A, El-Bary.A.A and Morsey.M.M, Space approach to the hydro-magnetic flow of a dusty fluid through a porous medium, Comput. Math. Appl., 59 (2010) 2868-2879.

[23] Attia.H.A, Al-kaisy.A.M.A and K.M.Ewis, MHD Couette Flow and Heat Transfer of a Dusty Fluid with Exponential Decaying Pressure Gradient, Tamkang J. of Scie. and Eng., 14 (2) (2011) 91-96.

[24] Gireesha B.J, Chamkha A.J, Manjunatha.S and Bagewadi C.S, Mixed convective flow of a dusty fluid over a vertical stretching sheet with non-uniform heat source/sink and radiation, Int. J. Numer. Meth. Heat Fluid Flow, 23(4) (2013) 598-612.

[25] Gireesha.B.J, Roopa.G.S and Bagewadi.C.S, Effect of viscous dissipation and heat source on flow and heat transfer of dusty fluid over unsteady stretching sheet, Appl. Math. Mech. -Engl. Ed., 33(8) (2012) 1001-1014.

[26] G. M. Pavithra, B. J. Gireesha. "Effect of viscous dissipation on hydromagnetic fluid f low and heat transfer in a porous medium at an exponentially stretching sheet with fluidparticle suspension", Afrika Matematika,(26) 419 - 432 2013

[27] Gowdara M. Pavithra, Bijjanal J. Gireesha. "Unsteady flow and heat transfer of a fluidparticle suspension over an exponentially stretching sheet", Ain Shams Engineering Journal, 5(2) 2014

[28] Yogeesh N, "Graphical representation of Solutions to Initial and boundary value problems Of Second Order Linear Differential Equation Using FOOS (Free & Open Source Software)-Maxima", International Research Journal of Management Science and Technology (IRJMST), 5(7), 2014, 168-176.

[29] Yogeesh N, "Solving Linear System of Equations with Various Examples by using Gauss method", International Journal of Research and Analytical Reviews (IJRAR), 2(4), 2015, 338-350